3D Structure of the Complex of MDL 63,246 with the Cell Wall Model Peptide Ac_2-Lys-D-Ala-D-Ala

Michael Kurz,*,† Wolfgang Guba,† and Bianca Patrizia Andreini

Contribution from the Lepetit Research Center, Hoechst Marion Roussel, Via R. Lepetit 34, 21040 Gerenzano (VA), Italy

Received November 27, 1995[⊗]

Abstract: The complex between the glycopeptide MDL 62,346 and the model cell wall analog Ac_2-Lys-D-Ala-D-Ala was studied by NMR spectroscopy in DMSO solution. A complete assignment of proton and carbon resonances was achieved, and the data were compared with the results observed for the free glycopeptide. NOE buildup rates were determined to calculate interproton distances which were used as constraints to model the 3D structure of the complex. Molecular dynamics simulations were performed in DMSO to gain further insight into the stability of the complex and the dynamical behavior of structural features. The structure of the glycopeptide backbone and the attractive interactions in the intermolecular interface are very well defined. The complex is stabilized by the formation of five intermolecular hydrogen bonds between the glycopeptide and the tripeptide.

Introduction

The vancomycin class of glycopeptide antibiotics has assumed increasing importance during the last 20 years. More recently an increase in serious infections caused by vancomycin-resistant enterococci has been observed in hospitalized patients.[1] Teicoplanin, the only other glycopeptide in clinical use, is active against some but not all vancomycin-resistant strains. Therefore, chemical modifications of teicoplanin and teicoplanin-like glycopeptides are an important step for the development of new antibiotics which are active toward highly-resistant enterococci.

The most interesting derivative which has been found so far is MDL 63,246,[2] a derivative of the teicoplanin-like antibiotic A-40,926[3,4] (see Figure 1). It is formed by reduction of the carboxyl group in the *N*-acylglucoronic acid followed by an amidation of the terminal carboxyl group with [3-(*N*,*N*-dimethylamino)propyl]amine. The compound shows in-vitro activity against strains of *Enterococcus faecalis* and *Enterococcus faecium* which are highly resistant to both vancomycin and teicoplanin.[2]

The mechanism of action for glycopeptides has been investigated for many years, and a model, at least for the first step of interaction, has been developed. The compounds interfere with the biosynthesis of bacterial cell walls by binding to mucopeptide precursors terminating in the sequence D-Ala-D-Ala. Much effort has been invested to study the interactions between model peptides containing the D-Ala-D-Ala sequence and glycopeptides on a molecular level.[5−20] A powerful technique for these investigations is NMR spectroscopy which has been used by several groups, especially the one of Dudley H. Williams who studied the complexes of vancomycin and Ristocetin A with Ac-D-Ala-D-Ala and Ac_2-Lys-D-Ala-D-Ala, respectively.[5−15]

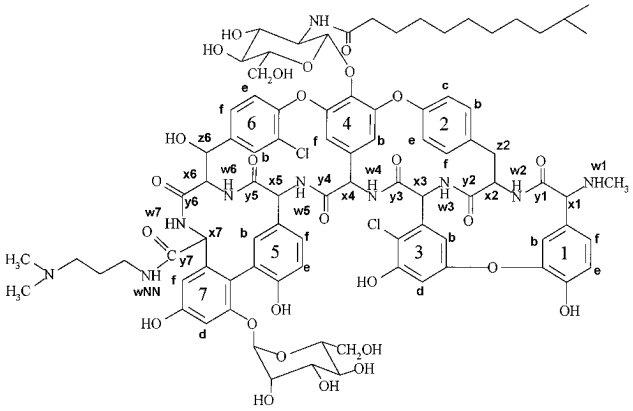

Figure 1. Structure of MDL 63,246.

* To whom correspondence should be addressed.

† Present address: Central Pharma Research, Hoechst AG, G-838, 65926 Frankfurt, Germany.

⊗ Abstract published in *Advance ACS Abstracts,* June 1, 1996.

(1) Johnson, A. P.; Uttley, A. H. C.; Woodford, N.; George, R. C. *Clin. Microbiol. Rev.* **1990**, *3*, 280−290.

(2) Malabarba, A.; Ciabatti, R.; Scotti, R.; Goldstein, B. P.; Ferrari, P.; Kurz, M.; Andreini, B. P.; Denaro, M. *J. Antibiot.* **1995**, *48*, 869−883.

(3) Waltho, J. P.; Williams, D. H.; Selva, E.; Ferrari, P. *J. Chem. Soc., Perkin Trans. 1* **1987**, 2103−2107.

(4) Goldstein, B. P.; Selva, E.; Gastaldo, L.; Berti, M.; Pallanza, R.; Ripamonti, F.; Ferrari, P.; Denaro, M.; Arioli, V.; Cassani, G. *Antimicrob. Agents Chemother.* **1987**, *31*, 1961−1966.

(5) Williams, D. H.; Kalman, J. R. *J. Am. Chem. Soc.* **1977**, *99*, 2768−2774.

(6) Kalman, J. R.; Williams, D. H. *J. Am. Chem. Soc.* **1980**, *102*, 906−912.

(7) Williams, D. H.; Butcher, D. W. *J. Am. Chem. Soc.* **1981**, *103*, 5697−5700.

(8) Williams, D. H.; Williamson, M. P.; Butcher, D. W.; Hammond, S. J. *J. Am. Chem. Soc.* **1983**, *105*, 1332−1339.

(9) Williamson, M. P.; Williams, D. H.; Hammond, S. J. *Tetrahedron* **1984**, *40*, 569−577.

(10) Williamson, M. P.; Williams, D. H. *Eur. J. Biochem.* **1984**, *138*, 345−348.

(11) Williamson, M. P.;Williams, D. H. *J. Chem. Soc., Perkin Trans. 1* **1985**, 949−956.

(12) Kannan, R.; Harris, C. M.; Harris, T. M.; Waltho, J. P.; Skelton, N. J.; Williams, D. H. *J. Am. Chem. Soc.* **1988**, *110*, 2946−2953.

(13) Waltho, J. P.; Cavanagh J.; Williams, D. H. *J. Chem. Soc., Chem. Commun.* **1988**, 707−709.

(14) Williams, D. H.; Waltho, J. P. *Biochem. Pharmacol.* **1988**, *37*, 133−141.

(15) Waltho, J. P.; Williams, D. H. *J. Am. Chem. Soc.* **1989**, *111*, 2475−2480.

(16) Brown, J. P.; Terenius, L.; Feeney, J.; Burgen, A. S. V. *Mol. Pharmacol.* **1975**, *11*, 119−125.

(17) Brown, J. P.; Terenius, L.; Feeney, J.; Burgen, A. S. V. *Mol. Pharmacol.* **1975**, *11*, 126−132.

(18) Convert, O.; Bongini, A.; Feeney, J. *J. Chem. Soc., Perkin Trans. 2* **1980**, 1262−1270.

(19) Fesik, S. W.; Armitage, I. M.; Ellestad, G. A.; McGahren, W. J. *Mol. Pharmacol.* **1984**, *25*, 281−286.

(20) Prowse, W. G.; Kline, A. D.; Skelton, M. A.; Loncharich R. *Biochemistry* **1995**, *34*, 9632−9644.

S0002-7863(95)03939-4 CCC: $12.00

For a better understanding of the structural requirements for an optimal binding of cell wall model peptides, we studied the complex between MDL 63,246 and Ac_2-Lys-D-Ala-D-Ala by NMR spectroscopy and molecular modeling. In the present paper we describe the complete assignment of all proton and carbon resonances and the three-dimensional structure which has been determined by molecular dynamics calculations using NOE distance constraints.

Experimental Methods

NMR Spectroscopy. All NMR spectra have been recorded on a Bruker AMX 600 at 30 °C. The complex was formed by adding Ac_2-Lys-D-Ala-D-Ala to a solution of 20 mg of MDL 63,246 in 0.5 mL of DMSO-d_6. The formation of the complex was monitored by the appearance of various significant resonances which belonged to the antibiotic or the tripeptide in the bound form (see the Results). For the signal assignment of the free tripeptide a solution of 20 mg in 0.5 mL of DMSO-d_6 has been used. The data were processed on an Aspect station with the UXNMR software from Bruker.

All homonuclear experiments (DQF-COSY,[21] TOCSY,[22] ROESY,[23] and NOESY[24]) were performed with a spectral width of 15 ppm (10 ppm for the free tripeptide). In all of the experiments, spectra were recorded with 512 increments in t_1 and 4096 complex data points in t_2. For the ROESY and NOESY 32 transients were averaged for each t_1 value, for COSY and TOCSY 16 transients. Mixing times of 70 and 150 ms were used for TOCSY and ROESY spectra, respectively. NOESY spectra were acquired with mixing times of 20, 40, 60, 80, 100, and 150 ms to determine NOE buildup rates.

For HMQC[25] spectra 512 increments (64 scans) with 2048 complex data points in t_2 were collected using a sweep width of 10 ppm in the proton dimension and 165 ppm in the carbon dimension. A BIRD pulse[26] was applied to suppress magnetization of protons connected to ^{12}C (recovery delay of 200 ms). The HMBC[27] spectra were acquired with a sweep width of 15 ppm in the proton dimension (10 ppm for the tripeptide) and 165 ppm in the carbon dimension. A total of 320 transients for the complex and 160 for the tripeptide were averaged for each of 512 increments in t_1, and 2048 complex points in t_2 were recorded. A delay of 3.3 ms was used to suppress $1 - J$ couplings, and 70 ms was taken for the development of long-range correlations. After Fourier transformation the strong t_1 noise was reduced by a mean row subtraction using the AURELIA program (Bruker).

Molecular Modeling. Molecular dynamics (MD) simulations and interactive modeling were performed with DISCOVER (consistent valence force field) and INSIGHT II from Biosym Technologies of San Diego, CA, and Tripos's Sybyl Version 6.1a on SGI 340/VGX, ONYX, and Cray YMP computers.

The starting structure of the complex was placed into a DMSO solvent box consisting of 890 DMSO molecules. The carboxylate group of the tripeptide was treated as charged; no counterion was included. After an energy minimization using conjugate gradients (10 000 iterations), a constrained MD simulation was initiated starting at 50 K. The interproton distances, which were obtained from buildup rates in NOESY spectra, were applied as distance restraints with a tolerance of 10% and with the usual pseudoatom corrections. The temperature was raised in 1 ps steps (integration step of 1 fs) by 50 K until 300 K was reached. The simulation was continued for 100 ps at this temperature to allow an equilibration of the system. Throughout the MD simulation, temperature and pressure (1.0 bar) bath coupling[29] was applied. Another 500 ps of restrained MD was carried out, and after every picosecond the structure was recorded, resulting in 500 structures which were used for further analysis. After the 500 ps, the simulation was carried on for 750 ps without distance constraints (in the following text termed as "free MD simulation"); structures were recorded every picosecond. This calculation should provide for insights into the structural stability of the complex and the dynamical behavior of the complex. Starting from the sample frame at 40 ps, a total of 6 structures in 140 ps intervals were energy-minimized in vacuo with 100 iterations of conjugate gradients, applying a distance dependent dielectric constant of 1.

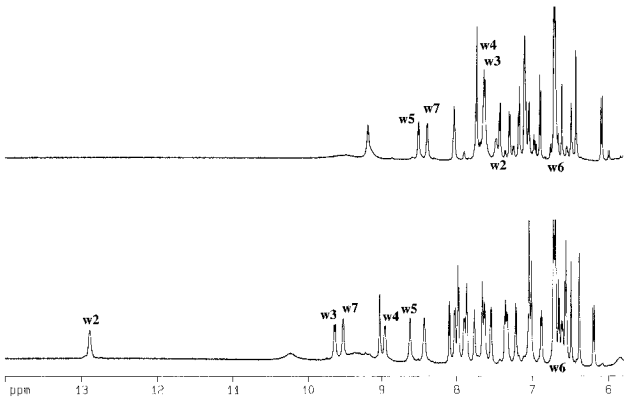

Figure 2. Amide region of the ^1H spectra of MDL 63,246 and of the complex between MDL 63,246 and diacetyl-Lys-D-Ala-D-Ala. The spectra were recorded in DMSO-d_6 at 30 °C at 600 MHz. The shifts of the amide protons upon complexation are indicated.

Results

Unfortunately, it was not possible to obtain well-resolved NMR spectra of MDL 63,246 in aqueous solutions, although many mixtures with different organic solvents at different pH values and temperatures have been tried. The same was true for the complex between MDL 63,246 and Ac_2-Lys-D-Ala-D-Ala. Therefore, we used DMSO-d_6 as solvent, which had also been used for the assignment of the free glycopeptide.[2] The complex was formed by adding Ac_2-Lys-D-Ala-D-Ala to a solution of MDL 63,246 in DMSO-d_6. The sharp resonances of the complex in the ^1H-NMR spectrum indicate that the free components and the complex are in a slow exchange on the NMR time scale, which is important for an accurate conformational analysis. In the case of vancomycin, the exchange rate in DMSO-d_6 is too fast, which results in very broad signals. Williams and co-workers circumwent this problem by adding 30% CCl_4 to the DMSO solution and lowering the temperature to 0 °C.[8] It is worthwhile to mention that also the aglycon of MDL 63,246 (without sugar moieties and with a free terminal carboxyl group[30]) showed this phenomenon of line broadening in DMSO after the addition of the tripeptide, indicating a significantly higher exchange with respect to the complete molecule.

The assignment of all proton and carbon resonances was carried out by following the same strategy already described for the free MDL 63,246.[2] The ^1H-NMR spectrum of the complex is characterized by drastic changes of some chemical shifts (see Figure 2) which were observed in all NMR studies of complexes between glycopeptides and di- or tripeptides containing the D-Ala-D-Ala terminus.[5−20] Tables 1 and 2 compare the chemical shifts of all proton and carbon resonances of MDL 63,246 and Ac-Lys-D-Ala-D-Ala in the free and in the bound forms.

(21) Derome, A.; Williamson, M. *J. Magn. Reson.* **1990**, *88*, 177−185.
(22) Bax A.; Davis, D. G. *J. Magn. Reson.* **1985,** *65*, 355−360.
(23) Bothner-By, A. A.; Stephens, R. L.; Lee, J.; Warren, C. D.; Jeanloz, J. W. *J. Am. Chem. Soc.* **1984**, *106*, 811−813.
(24) Jeener, J.; Meier, B. H.; Bachmann, P.; Ernst, R. R. *J. Chem. Phys.* **1979**, *71*, 4546−4553.
(25) Bax, A.; Subramanian, S. *J. Magn. Reson.***1986**, *67*, 565−569.
(26) Garbow, J. R.; Weitkamp, D. P.; Pines, A. *Chem. Phys. Lett.* **1982**, *93*, 504−509.
(27) Bax, A.; Summers, M. F. *J. Am. Chem. Soc.* **1986**, *108*, 2093−2094.
(28) Kurz, M.; Guba, W. Unpublished results.
(29) Berendsen, H. J. C.; Postma, J. P. M.; van Gunsteren, W. F.; DiNola, A.; Haak, J. R. *J. Chem. Phys.* **1984**, *81*, 3684−3690.
(30) Selva, E.; Goldstein, B. P.; Ferrari, P.; Pallanza, R.; Riva, E.; Berti, M.; Borghi, A.; Beretta, G.; Scotti, R.; Romanó, G.; Cassani, G.; Arioli,V.; Denaro, M. *J. Antibiot.* **1988**, *41*, 1243−1252.

Table 1. ^{1}H and ^{13}C Chemical Shifts of MDL 63,246 in the Free and in the Bound Forms[a]

	free		bound			free		bound	
	^{1}H	^{13}C	^{1}H	^{13}C		^{1}H	^{13}C	^{1}H	^{13}C
1-CH_3	2.33	34.1	2.43	31.0	5f	6.71	125.8	6.69	125.6
x1	4.31	66.1	4.91	63.1	w6	6.69		6.62	
y1		172.2		167.7	x6	4.13	62.1	4.34	52.7
1a		129.3		123.0	y6		168.0		167.2
1b	6.60	115.9	6.48	119.4	z6	5.19	71.5	5.00	72.1
1c		142.6		142.3	6a		141.9		141.5
1d		146.3		148.3	6b	7.73	127.1	7.01	127.6
1e	6.89	117.5	6.56	116.4	6c		126.1		126.0
1f	7.04	124.7	6.87	127.6	6d		148.6		148.5
w2	7.47		12.89		6e	7.30	123.4	7.22	123.1
x2	4.91	54.4	5.04	55.1	6f	7.43	126.9	7.36	126.4
y2		169.2		169.7	w7	8.39		9.56	
z2	3.33/2.81	37.4	3.32/2.78	37.9	x7	4.41	57.3	4.82	56.0
2a		133.3		133.1	y7		169.8		171.0
2b	7.10	130.6	7.03	130.0	7a		137.4		136.2
2c	7.18	124.1	7.03	123.1	7b		120.2	6.72	119.9
2d		154.7		154.5	7c		154.3		156.8
2e	7.09	122.6	6.70	122.3	7d	6.71	101.0	6.38	100.7
2f	7.62	131.1	7.54	132.9	7e		157.2		154.4
w3	7.63		9.65		7f	6.42	108.0		108.4
x3	6.08	53.8	6.19	54.2	w-NN	8.03		8.44	
y3		167.5		167.7	NNa	3.19	37.5	3.29/3.15	36.8
3a		138.5		139.9	NNb	1.62	26.6	1.68	26.8
3b		114.2		118.3	NNc	2.30	57.0	2.48	56.0
3c		154.4		153.8	NNd	2.17	44.9	2.32	44.3
3d	6.69	107.4	6.68	105.9	AG-NH	7.74		7.65	
3e		154.6		156.9	AG1	5.32	102.1	5.19	102.7
3f	6.48	107.1	6.55	107.0	AG2	3.70	56.2	3.63	56.3
w4	7.64		8.97		AG3	3.60	73.7	3.59	73.6
x4	5.65	54.9	5.68	53.7	AG4	3.22	70.6	3.30	70.5
y4		169.9		170.6	AG5	3.19	77.2	3.06	76.7
4a		133.5		133.9	AG6	3.72	61.4	3.58	60.9
4b	5.78	108.3	5.60	107.6	M1	5.25	96.8	5.01	96.7
4c		153.7		153.8	M2	3.22	70.8	2.99	70.9
4d		133.0		133.1	M3	3.22	69.7	3.17	69.0
4e		151.5		151.3	M4	3.48	66.1	3.41	65.9
4f	5.12	103.9	5.06	103.53	M5	3.48	73.8	2.99	73.4
w5	8.50		8.63		M6	3.51	60.8	3.51	60.8
x5	4.42	53.6	4.66	53.6	FA1		172.1		172.1
y5		169.2		169.8	FA2	2.00	36.0	1.94	35.9
5a		125.2		124.9	FA3	1.40	25.0	1.37	25.0
5b	7.10	135.3	7.66	136.2	FA4−FA9	1.00−1.20	29.3−28.7	1.00−1.20	29.3−28.7
5c		120.9		121.2	FA10	1.49	27.4	1.49	28.2
5d		155.2		155.1	FA11, FA12	0.85	22.5	0.85	22.5
5e	6.71	116.1	6.65	115.5					

[a] Recorded in DMSO-d_6 at 303 K. Chemical shifts are referenced to DMSO (2.50 and 39.5 ppm, respectively).

The drastic changes of the chemical shifts for four of the seven secondary amide protons (w2, w3, w4, and w7) upon binding of Ac_2-Lys-D-Ala-D-Ala to MDL 63,246 have been observed for other glycopeptides in organic solvents[6−8,10] as well as in aqueous solution.[11,19,20] This fact was explained by the formation of intermolecular hydrogen bonds between the terminal carboxylate group of the cell wall model peptide and the amide protons w2, w3, and w4 of the glycopeptides. Additionally, w7 is forming a hydrogen bond with the carbonyl group of the preceding D-Ala residue. The strength of these hydrogen bonds was directly correlated to the size of the downfield shift in amide proton frequencies.[10]

To confirm the pattern of hydrogen bonds, the temperature coefficients of the amide protons of MDL 63,246 and of the tripeptide in the free and bound forms were determined by measuring ^{1}H-NMR spectra at 300, 310, 320, and 330 K. Those protons which are exposed to the solvent should show a higher temperature dependency of their chemical shifts than those which are involved in intra- or intermolecular hydrogen bonds.[6,11] The results are shown in Table 3. It can be seen that most of the amide protons which are expected to be involved in intermolecular hydrogen bonds (w2, w3, w4, and Ala^3-NH) have temperature coefficients smaller than $-3 \times 10^{-3}\delta/T$ (ppm/K). However, the amide proton w7 which should also form an intermolecular hydrogen bond with the α-carboxyl group of the lysine residue shows a very high temperature coefficient. Additionally, the temperature coefficients of w2 and w7 are smaller in the free glycopeptide than in the complex, although no hydrogen bonds are formed in the free form. Therefore, the structural relevance of this parameter is not clear.

Although the changes of the chemical shifts for the other protons are less dramatic than those observed for the amide protons, some of them are still significant. The protons x1 and x7 experience downfield shifts of 0.60 and 0.41 ppm, respectively. For the other H^α-protons downfield shifts of 0.03 (x4), 0.11 (x3), 0.13 (x2), 0.21 (x6), and 0.24 ppm (x5) are observed. Among the aromatic protons 5b experiences a drastic downfield shift whereas 1e, 2e, 6b, and 7d are shifted toward higher field. Table 1 reveals that also the anomeric protons of both sugar residues experience upfield shifts of 0.13 ppm (AG1) and 0.25 ppm (M1), respectively. The same is true for most of the other sugar protons, especially M2 (+0.23 ppm) and M5 (+0.49 ppm).

In the case of the tripeptide the resonances of the two methyl groups of the alanine residues experience a strong upfield shift

Table 2. ^{1}H and ^{13}C Chemical Shifts of Ac_2-Lys-D-Ala-D-Ala in the Free and in the Bound Forms[a]

	free		bound	
	^{1}H	^{13}C	^{1}H	^{13}C
Lys^1-NH	8.00		7.91	
Lys^1-α	4.18	52.7	4.48	51.9
Lys^1-*β*	1.57/1.47	31.5	1.36	30.8
Lys^1-*γ*	1.25/1.19	22.8	1.37/1.29	23.4
Lys^1-*δ*	1.36	28.8	1.47	28.2
Lys^1-*ϵ*	2.98	38.3	3.08	38.6
Lys^1-*ϵ*-NH	7.78		7.87	
Lys^1-C′		171.4		172.7
α-Acetyl	1.83	22.4	1.97	22.5
α-Acetyl-C′		169.4		169.8
ϵ-Acetyl	1.78	22.60	1.85	22.5
ϵ-Acetyl-C′		168.9		169.2
D-Ala^2-NH	8.14		8.05	
D-Ala^2-α	4.30	47.6	4.49	48.4
D-Ala^2-*β*	1.19	18.1	0.85	19.7
D-Ala^2-C′		171.8		169.8
D-Ala^3-NH	8.08		7.33	
D-Ala^3-α	4.16	47.4	3.82	49.3
D-Ala^3-*β*	1.28	17.0	0.50	19.7
D-Ala^3-C′		173.9		175.1

[a] Recorded in DMSO-d_6 at 303 K. Chemical shifts are referenced to DMSO (2.50 and 39.5 ppm, respectively).

Table 3. Temperature Coefficients of MDL 63,246 and Ac_2-Lys-D-Ala-D-Ala[a]

proton	free	bound
w2	0.9	3.0
w3	3.1	2.3
w4	5.4	1.3
w5	5.3	6.0
w6	4.4	5.3
w7	3.1	7.3
wNN	7.3	9.0
AG-NH	5.7	6.7
Lys^1-α-NH	4.8	4.0
Lys^1-*ϵ*-NH	5.0	6.3
Ala^2-NH	6.6	6.7
Ala^3-NH	5.0	0.0

[a] Temperature coefficients are given by $-3 \times 10^{-3}\ \delta/T$ (ppm/K). Chemical shifts were obtained at 300, 310, 320, and 330 K.

which was firstly observed by J. P. Brown et al.[16,17] Especially the methyl group of the terminal alanine residue (Ala^3) undergoes a large upfield shift (0.78 ppm) which was explained by the orientation of this group perpendicular to one of the aromatic rings. However, also some of the other resonances experience a considerable change in their chemical shifts including all three α-protons and the amide proton of Ala^3 (see Table 2). The last one is also characterized by a very low temperature coefficient which might indicate the participation of this proton in an intermolecular hydogen bond with the glycopeptide.

Conformational Analysis

Determination of NOE Distance Restraints. The 3D structure of the complex was determined by restrained molecular dynamics (MD) simulations using interproton distances derived from NOESY spectra (supporting information, Figure I). The integration of six spectra with mixing times of 20, 40, 60, 80, 100, and 150 ms revealed that the buildup rates of the NOEs were linear only up to 80 ms. The integral values of the spectra with mixing times of 100 and 150 ms were clearly affected by spin diffusion. Therefore, only the first four NOESY spectra were used for the determination of the buildup rates. The strong NOE between x5 and x6, which is due to the cis configuration of the corresponding peptide bond, was used for the calibration of all other distances by setting it to 1.8 Å. A total of 113 restraints could be assigned including 36 intermolecular restraints between the glycopeptide and the tripeptide. All interproton distances are listed in Table 1 of the supporting information.

Table 4. *J*(HN−Hα) Coupling Constants for MDL 63,246 and the Aglycon[a]

amide proton	MDL 63,246 (free)	MDL 63,246 (bound)	aglycon
w2	broad	9.3	9.3
w3	10.6	10.1	10.6
w4	8.0	8.6	8.0
w5	5.7	4.5	5.3
w6	11.5	11.5	11.9
w7	6.2	6.5	6.0

[a] Coupling constants given in hertz. Recorded in DMSO at 303 K.

Generation of the Starting Structure. The analysis of the NOESY spectra revealed 72 correlations between protons of the glycopeptide. Although the chemical shifts of many protons had changed significantly, the NOE pattern itself was very similar to those obtained for the free glycopeptide and for the aglycon.[28] This observation indicated that the conformation of the glycopeptide did not change significantly due to the formation of the complex. Furthermore, a comparison of the *J*(HN−Hα) coupling constants of the free and bound forms of MDL 63,246 with those obtained for the aglycon confirmed the conformational similarity of the peptide core (Table 4).

Considering these experimental results, the 3D structure of the aglycon which had been determined previously[28] was chosen as a starting structure for the glycopeptide in the complex. Although the number of NOEs between protons of the tripeptide is limited due to spectral overlap of the α-protons of Lys^1 and Ala^2, an extended structure could be deduced from the available data. The tripeptide was manually docked to the glycopeptide, taking into account the models published by Williams et al.

Analysis of the Trajectories. Using 113 distance constraints, a restrained molecular dynamics simulation was carried out over 500 ps followed by a free simulation over 750 ps (see the Experimental Methods). In Table 1of the supporting information, the averaged interproton distances of both simulations are compared with the experimental distances. Considering the limits which were used for each restraint during the calculation (see the Experimental Methods), almost all interproton distances were in accordance with the experimental data. Comparing the results of the restrained simulation with those of the free one, no significant differences could be observed except for the distance wNN/x7. In this case the result of the free simulation is closer to the experimental value than the distance obtained in the restrained simulation. An explanation will be given in the following.

In Table 5 the averaged backbone dihedral angles are listed. As already observed for the interproton distances, the results of the two simulations are very similar. It should be pointed out that the glycopeptide backbone is very rigid during both simulations. This is illustrated in Figure 3 which shows a superposition of six structures taken from the trajectory of the free simulation (see the Experimental Methods). The pairwise rms deviation of all heavy atoms of the peptide core including the aromatic side chains is given in Table 6. The analysis of the *ψ*-angle of residue 7 in the free simulation, however, demonstrates that this dihedral angle occupies two different conformational states (Figure 4). This conformational transition which was not observed during the restrained simulation leads to the difference in the interproton distance between wNN and x7.

Table 5. Backbone Dihedral Angles[a]

residue	Φ (res)	Φ (free)	ψ (res)	ψ (free)	ω (res)	ω (free)
1			−155(13)	−150(13)	−175(5)	−176(6)
2	102(13)	97(13)	39(10)	42(11)	−169(6)	−169(6)
3	−151(9)	−148(15)	−12(20)	−52(12)	175(5)	175(6)
4	119(12)	121(13)	−136(9)	−132(12)	−160(5)	−159(6)
5	143(10)	139(13)	−148(9)	−146(10)	3(11)	3(12)
6	−104(9)	−102(9)	134(8)	130(8)	−148(7)	−152(7)
7	−80(8)	−79(9)	−27(20)	50(80)	180(12)	180(11)

[a] The dihedral angles (deg) are the average values over a trajectory of 500 ps restrained MD ("res") and 750 ps free MD ("free"). The standard deviation is given in parentheses.

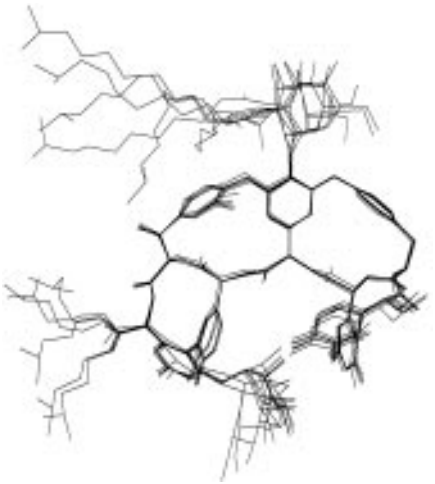

Figure 3. Superposition of six minimized structures from the trajectory of the free MD simulation in 140 ps intervals starting from 40 ps. All heavy atoms of the peptide core were taken as reference points. The tripeptide is not shown for the sake of clarity.

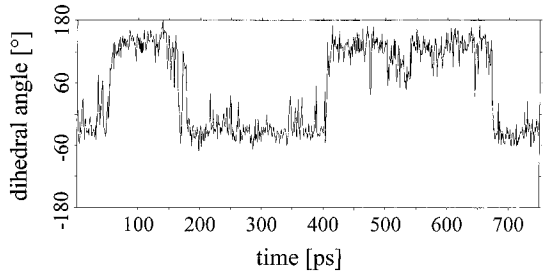

Figure 4. Time course of the ψ angle of residue 7 of the glycopeptide during the free MD simulation. The dihedral angle occupies two different conformational states.

In contrast to the rigid core, the orientation of the fatty acid chain and the 3-(*N*,*N*-dimethylamino)propyl amide group undergo significant changes during the simulation (see Figure 3). Both of these substituents are, in principle, able to form hydrophobic interactions with the lysine side chain, but no stable hydrophobic clustering could be observed during the simulation. Also the sugar moieties do not seem to be involved in the binding of the tripeptide. The two alanine residues are kept in their position, whereas the N-terminal lysine shows a high degree of flexibility. This is shown in Figure 5, where the same structures as in Figure 3 together with the bound tripeptide are depicted according to the time course of the trajectory.

Another important structural feature is the intermolecular hydrogen bonds between the glycopeptide and the tripeptide. A graphical presentation of the corresponding proton−acceptor distances during the free simulation is given in Figure 2 of the supporting information for all intermolecular hydrogen bonds. Table 7 contains the average distances and the corresponding standard deviations. It must be pointed out that also for w7 and the carbonyl oxygen of Lys a very strong interaction is obtained (with and without constraints), although a high temperature coefficient is observed for w7.

Table 6. RMS Comparison of the Peptide Core of MDL 63,246 over the Free MD Trajectory[a]

	40 ps	180 ps	320 ps	460 ps	600 ps	740 ps
40 ps		0.375	0.276	0.241	0.270	0.513
180 ps			0.351	0.436	0.420	0.752
320 ps				0.312	0.331	0.538
460 ps					0.211	0.460
600 ps						0.559

[a] The values correspond to the pairwise RMS deviation (Å) of the six structures shown in Figures 3 and 5. Atoms included are all heavy atoms of the glycopeptide core without [3-(*N*,*N*-dimethyamino)propyl]-amine, the sugars, and the fatty acid.

Table 7. Intermolecular Hydrogen Bonds[a]

donor	acceptor	MD (res)	MD (free)
w2	Ala^3-CO(1)[b]	2.51(0.21)	1.89(0.16)
w3	Ala^3-CO(2)[b]	2.06(0.17)	2.04(0.18)
w4	Ala^3-CO(2)[b]	1.88(0.16)	1.97(0.23)
Ala^3-NH	y4	2.40(0.22)	2.43((0.32)
w7	Lys^1-C′	1.96(0.16)	2.14(0.27)

[a] The distances (Å) are the average values over a trajectory of 500 ps restrained MD ("res") and 750 ps free MD ("free"). The numbers in parentheses correspond to the standard deviation. [b] CO(1) and CO(2) correspond to the two oxygens of the carboxylate group of Ala^3.

Characterization of the Binding Interface. Figure 6 shows the sterical complementarity between the glycopeptide and the tripeptide cell wall analog. The close match of the two molecular surfaces prevents the final transpeptidation step to yield the rigid peptidoglycan wall. The main factor in determining the strength of the interaction between MDL 62,346 and the tripeptide is the hydrogen bonds at the interface which are essentially the same as observed by Williams et al. The fairly rigid structure of the glycopeptide backbone exposes amide protons and carbonyl oxygens in such a way as to provide for optimum interactions with the tripeptide in an extended conformation (Figure 7).

Besides the intermolecular hydrogen bonds, hydrophobic interactions between the aromatic rings and the alanine side chains play an important role in the stability of the complex, as will be illustrated by the GRID approach.[31−34] In the GRID program the target, i.e., the glycopeptide, is placed onto a 3D grid. For the characterization of hydrophobic interactions, a methyl probe is placed at each grid point and the interaction energy between the probe and the target is calculated. By contouring the intersection points of calculated energies at negative energy levels, energetically favorable interaction sites with a methyl probe can be identified. In Figure 8, the regions where a methyl probe has a maximum interaction energy of −3 kcal/mol are depicted by solid-rendered contours and almost coincide with the alanine side chains. Thus, the glycopeptide core provides for optimum sterical, polar, and hydrophobic complementarity to ensure a tight binding of the tripeptide.

Conclusion

The solution structure of the complex between the glycopeptide MDL 62,346 and the model cell wall analog Ac_2-Lys-

(31) Goodford, P. J. *J. Med. Chem.* **1989**, *32*, 1083−1094.
(32) Boobbyer, D. N. A.; Goodford, P. J.; McWhinnie, P. M.; Wade, R. C. *J. Med. Chem.* **1989**, *32*, 1083−1094.
(33) Wade, R. C.; Clerk, K. J.; Goodford, P. J. *J. Med. Chem.* **1993**, *36*, 140−147.
(34) Wade, R. C.; Goodford, P. J. *J. Med. Chem.* **1993**, *36*, 148−156.

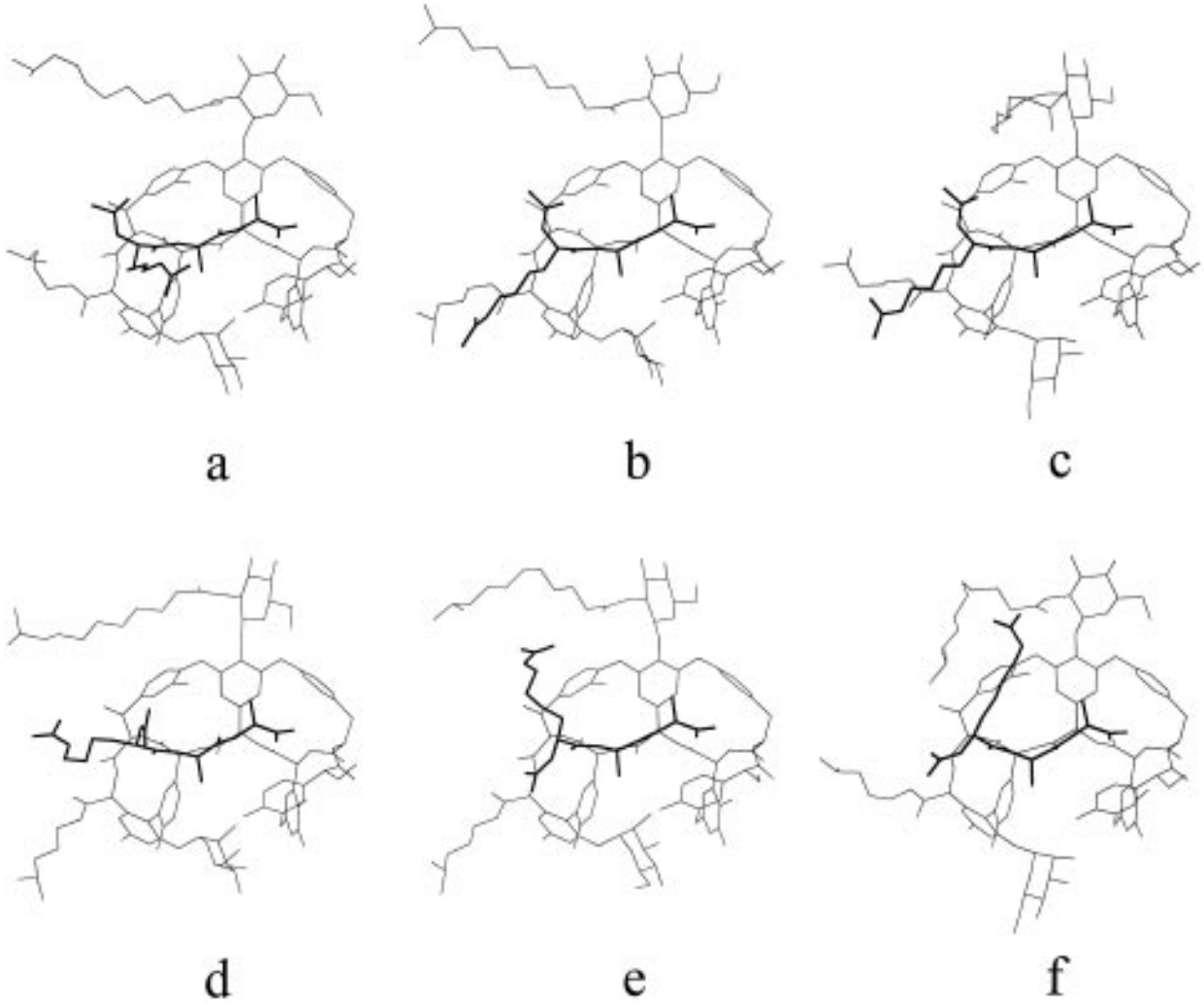

Figure 5. Six minimized structures from the trajectory of the free MD simulation: (a) after 40 ps, (b) after 180 ps, (c) after 320 ps, (d) after 460 ps, (e) after 600 ps, (f) after 740 ps. The tripeptide is shown in bold lines.

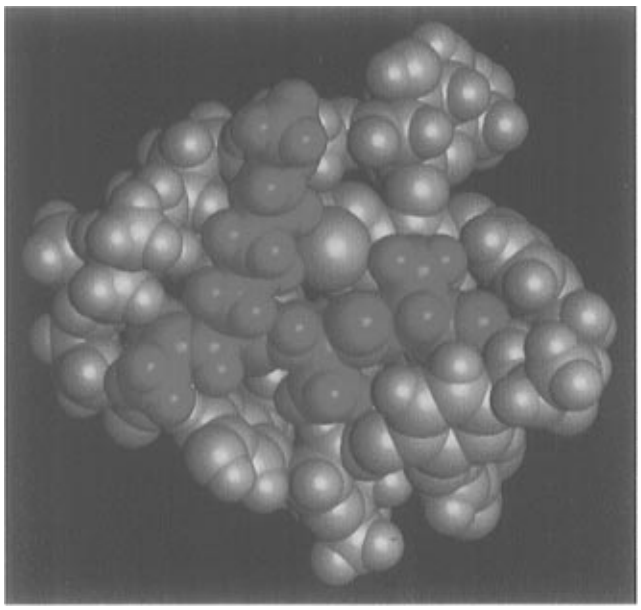

Figure 6. Space-filling model of MDL 63,246 (blue) and the tripeptide (red).

D-Ala-D-Ala was studied by NMR spectroscopy in DMSO. Interproton distances derived from NOESY spectra were used as constraints to model the 3D structure of the complex. Molecular dynamics simulations were performed in a DMSO solvent box to gain further insight into the stability of the complex and the dynamical behavior of structural features.

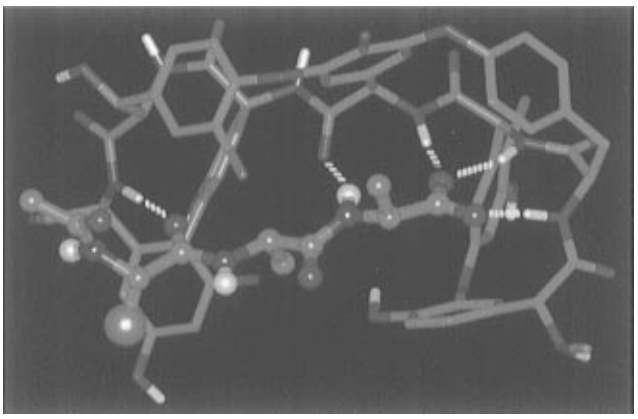

Figure 7. Intermolecular hydrogen bonds in the complex between MDL 63,246 and diacteyl-Lys-D-Ala-D-Ala. For the sake of clarity only the peptide core is shown (sticks). The tripeptide is shown in balls and sticks; the side chain of Lys is represented by an enlarged cpk.

The structure of the glycopeptide backbone is very rigid and does not undergo any significant structural changes upon binding. The attractive interactions in the intermolecular

(35) Bugg, T. D. H.; Wright, G. D.; Dutka-Malen, S.; Arthur, M.; Courvalin P.; Walsh, C. T. *Biochemistry* **1991**, *30*, 10408−10415.
(36) Arthur, M.; Courvalin, P. *Antimicrob. Agents Chemother.* **1993**, *37*, 1563−1571.

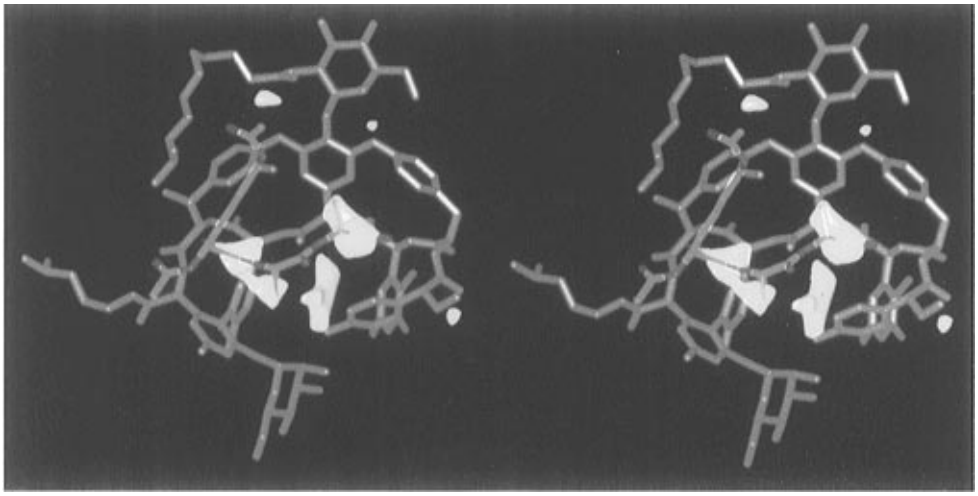

Figure 8. Energetically favorable interaction sites for a methyl probe on MDL 63,346 displayed as yellow, solid-rendered contours (contoured at -3 kcal mol^{-1}). The tripeptide was overlaid to show the common positions of the contours and the D-Ala side chains.

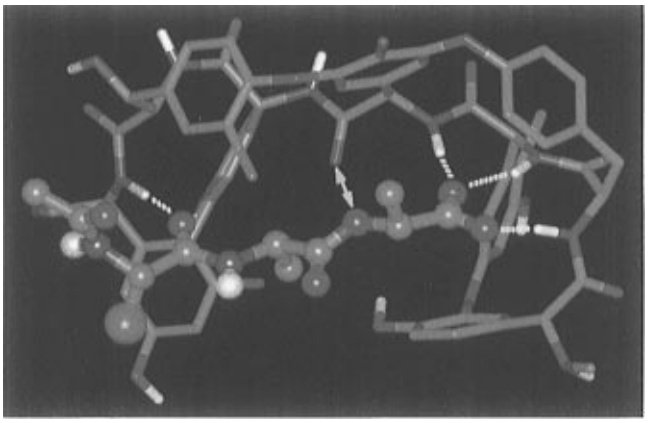

Figure 9. The terminal D-Ala was replaced with D-lactate by interactive modeling. For the sake of clarity only the peptide core is shown (in sticks). The tripeptide is shown in balls and sticks; the side chain of Lys is indicated by an enlarged cpk.

interface are very well defined by numerous intermolecular NOEs. The complex is stabilized by five intermolecular hydrogen bonds between the glycopeptide and the tripeptide. These hydrogen bonds are stable throughout the complete MD simulations, both with and without restraints. In addition, the hydrophobic interactions between the glycopeptide core and the two methyl groups of the alanine residues play an important role in the stability of the complex.

The model obtained from these studies also explains the molecular basis of resistance toward VanA enterococci where D-Ala-D-Ala is replaced by D-Ala-D-lactate.[35,36] On the one hand, the former hydrogen bond between the carbonyl oxygen y4 and the amide proton of D-Ala^3 would no longer exist, and on the other hand, this attractive element would be replaced by a repulsive interaction between y4 and the ester oxygen of D-lactate (Figure 9). Thus, a stable complex between D-Ala-D-lactate and MDL 63,246 (or any other glycopeptide of the vancomycin class) cannot be formed. This was confirmed by binding studies using UV and NMR spectroscopy.[37] These structural findings are in contrast to the observed activity of MDL 63,246 against vancomycin-resistant enterococci.[2] Therefore, other factors such as additional interactions with either proteins involved in the bacterial cell wall synthesis or the corresponding expression/translation systems might be involved.

Supporting Information Available: Table giving the interproton distances from NMR and MD and figures showing the time course of the intermolecular hydrogen bonds and NOESY spectrum of the complex between MDL 63,246 and diacetyl-Lys-D-Ala-D-Ala (5 pages). Ordering information is given on any current masthead page.

JA9539397

(37) Andreini, B. P. Unpublished results.